

Optimal control of grid-connected microgrid PV-based source under partially shaded conditions

A. Guichi ^{a, b, *}, S. Mekhilef ^{b, e, **}, E.M. Berkouk ^c, A. Talha ^d

^a Electrical Engineering Laboratory, Faculty of Technology, University Med Boudiaf of M'sila, Algeria

^b Power Electronics and Renewable Energy Research Laboratory (PEARL), Department of Electrical Engineering, University of Malaya, Kuala Lumpur, Malaysia

^c Laboratoire de Commande de Processus, ENP Alger, Algeria

^d Laboratoire d'instrumentation, USTHB Alger, Algeria

^e School of Software and Electrical Engineering, Swinburne, Victoria, Australia

ARTICLE INFO

Article history:

Received 29 June 2020

Received in revised form

30 March 2021

Accepted 13 April 2021

Available online 28 April 2021

Keywords:

Microgrid

Distributed generation unit

Grid-connected PV system

Maximum power point tracking (MPPT)

PSO

Intermediate power point tracking (IPPT)

Partial shading

ABSTRACT

Microgrids are gaining increasing attention globally and becoming increasingly powered by photovoltaic (PV) systems, thereby requiring high-efficiency control to function as a microgrid distributed generation unit. Accordingly, this study presents an optimal control of a grid-connected Microgrid PV Source (MPVS) under partially shaded conditions. The objective is to ensure the MPVSs ability to rapidly and precisely deliver the amount of power assigned by the supervisory controller. Thus, MPVS must shift rapidly and smoothly between the maximum and intermediate power point modes. The proposed system is composed of PV array, grid emulators, and two converters coupled to a common DC bus. The control strategy of the boost converter is based on the combination of two algorithms: particle swarm optimization algorithm and the proposed intermediate power point tracker algorithm. The voltage source inverter is controlled to keep the DC bus voltage constant and inject the power to the grid, in which the voltage-oriented control technique is applied and combined with the phase-locked loop algorithm for voltage synchronization. Lastly, all control algorithms are implemented in a DSpace 1104 environment and largely tested under various partially shaded patterns.

© 2020 The Author(s). This is an open access article under the CC BY-NC-ND license (<http://creativecommons.org/licenses/by-nc-nd/4.0/>).

1. Introduction

Electrical energy has become thrust engine of modern life, thereby pushing the electricity demand to increase with the electrification of our daily life activities. However, the electrical power sector is facing the depletion of fossil fuel reserves and the exigencies to reduce the emission of harmful gases [1,2]. Hence, the authors in Ref. [3] concluded that only with fully renewable energy (RE) system scenarios can our modern life meet the vast environmental, socioeconomic, and ethical sustainability demands of future electrical power systems. However, renewable energy sources suffer from intermittent power output, which is a challenging problem that should be solved to achieve rapid growth rate.

In small-scale power systems, this problem can be solved by the insertion of energy storage devices. However, this solution often results in significant RE cost increase [4], which will directly affect the development pace of these clean sources. Another efficient solution is to benefit from the complementarity of the generation patterns of different RE sources to reduce variability in the aggregate production. Hence, microgrids are cutting-edge technology capable of integrating and hybridizing different RE sources in the most reliable manner. This advantage is due to their advanced control capabilities and flexibility, apart from their wide range of benefits, such as their capability to disconnect from the traditional grid and operate autonomously [5]. Microgrids are mainly composed of renewable distributed generation units, typically solar and wind, and commonly reinforced with gas-fired generators and energy storage systems [6]. This resource mix makes microgrids considerably resilient to disruptions in fuel supply chains or to weather events that may impact renewable generation [7].

Among the renewable generations, the photovoltaic (PV) resource, owing to its ease of installation, long-term operation,

* Corresponding author. Electrical Engineering Laboratory, Faculty of Technology, University Med Boudiaf of M'sila, Algeria.

** Corresponding author.

E-mail addresses: amar.guichi@univ-msila.dz (A. Guichi), saad@um.edu.my (S. Mekhilef), emberkouk@yahoo.fr (E.M. Berkouk), abtalha@gmail.com (A. Talha).

local availability, and minimal maintenance, is an important sustainable distributed generation source [8]. To enhance the role of the PV resource as a DG unit in microgrids, its ability to adapt to the changing working mode and providing the requested power by the microgrid's supervisory must be ensured by an efficient control strategy. The extremely efficient method of using a PV source should be controlled to work on its maximum power point (MPP). Owing to the volatility and intermittent nature of renewable generation, the uncertainties in the load profiles, and protection of storage systems against overcharging, supervisors of microgrids continuously assign new reference power to distributed generation units to maintain the balance between load and generated power. This situation pushes the PV source to operate below MPP to fulfill the supervisory controller requirements. The power point that comes below MPP is called intermediate power point (IPP). Therefore, MPP is considered the most efficient power point, whereas IPP is the inescapable power point required by microgrids' supervisor under special operating conditions.

In the literature, MPP tracking has been extensively studied, particularly under partially shaded conditions, in which specific methods are used to track the global maximum power point (GMPP) because conventional algorithms (e.g., perturb and observe (P&O), hill climbing (HC), incremental conductance (INC)) may be simply stuck to one of the local maxima (LM). Different techniques based on artificial intelligence, such as fuzzy logic control (FLC) and artificial neural network (ANN), have been used to track GMPP. However, these methods require massive training and broad experience in a complex environment. Alternatively, recent studies have exhibited special interest on the bio-inspired MPPT algorithms, particularly swarm intelligence-based algorithms that have given better results than evolutionary algorithms [9]. Numerous studies have tested and evaluated these techniques under partial shading conditions (PSC), particle swarm optimization (PSO) [10], grey wolf optimization (GWO) technique [11], deterministic/dynamic cuckoo search algorithm (DCSA) [12,13], memetic salp swarm algorithm (MSSA) [14], artificial bee colony (ABC) [15], firefly algorithm (FA) [16], and ant colony optimization (ACO) [17]. Moreover, to enhance their performances and eliminate their drawbacks, several studies have integrated these algorithms into hybrid optimization methods, particularly by collaborating the optimization ability of various searching mechanisms as developed in Ref. [18] or into a combined forms of at least two techniques to compensate for the shortcomings of one technique by the performances of another [19,20]. Nevertheless, only few studies [21–26] have briefly mentioned the IPP achievement and they are limited to specific cases under a uniform insolation. To date, no algorithm has been developed to track IPP under partially shaded conditions, as is the case for GMPP, despite the crucial role of IPP in allowing the PV source to reach any reference power lower than MPP/GMPP. This situation will give the PV source the ability to meet all the microgrid supervisory controller exigency and enhance its significant role in this emerging system. In view of these shortcomings, the contribution of this study is to propose an efficient dual mode control strategy, which will allow the grid-connected microgrid PV source (MPVS) to switch smoothly and rapidly between two modes (i.e., maximum power mode (MPM) and intermediate power mode (IPM)) under any weather operating conditions. MPVS has been principally controlled to operate in MPM, through the application of the PSO algorithm, which has proven its superiority in speed convergence and implementation simplicity compared with other meta-heuristic optimization techniques [27] and guarantees less computational burden in contrast with their combined forms [28]. Once the power generated by the microgrid exceeds the total load demand and the storage system (if it exists) is fully charged, the microgrid supervisory controller urges the various units to

minimize their power according to the adopted strategy. Consequently, MPVS is obliged to shift to IPM. At this stage, the intermediate power point tracker (IPPT) algorithm, which we developed for the PV source in Ref. [29] is applied to reach the appropriate intermediate power level under uniform or partially shaded conditions. The second objective of this study is to inject the extracted/excess power to the utility grid. This process can be done either by using the one-stage system, in which only the three-phase VSI is interconnected between the PV array and grid; or by utilizing the two-stage system, in which the first stage converter is used to boost the PV array voltage and track the maximum operating point, then it comes the role of the three-phase VSI to convert the DC output of the first stage into an AC voltage [30]. Note that the one-stage system is of simple and considerably efficient topology, along with its new effective developed control strategies [31]. However, this study adopts the two-stage topology owing to the common sharing of the MPVS DC bus with other distributed generation units or distributed energy storage systems. Therefore, the boost converter is controlled to track either MPP/GMPP or IPP, whereas the grid-interfacing inverter is controlled to maintain a constant DC bus voltage and convert it into an AC voltage. To deliver the MPVS power to the grid/microgrid, the output voltage of the three-phase VSI should be synchronized with that of the latter as an imperative condition to grid-connected systems. The detailed description of the control schemes used will be provided in the succeeding section.

The remainder of this paper is arranged as follows. Section 2 briefly discusses an overview of the microgrid design, management, and control. Section 3 describes the power management strategy within a microgrid. Section 4 presents the characteristics and behavior of a PV array under uniform and partially shaded conditions. Section 5 provides the detailed description of the proposed system. Section 6 presents the control algorithms and strategies. Section 7 presents the experimental results. Lastly, Section 8 concludes this research.

2. Review of microgrid design, management, and control

To reduce the pressure on regional and national power utility grids, which continue to increase over the years, cities around the world has started to use microgrids that can contribute significantly to achieve energy production targets. The US Department of Energy [32] defines a microgrid as “a group of interconnected loads and Distributed Energy Resources (DERs) within clearly defined electrical boundaries that acts as a single controllable entity with respect to the grid to enable it to operate in both grid-connected or islanded modes.” This definition indicates that DERs with clearly defined electrical boundaries, a centralized supervisory controller that controls the entire system (DERs and loads), and being able to guarantee load power demand without the need for power grids could be considered a microgrid [6]. On the bases of these characteristics that determine the components, control methods, and power requirements of microgrids, Fig. 1 shows the general microgrid structure and its hierarchical control technique. Microgrids mainly comprise DERs, loads, centralized/distributed controllers, switches, and communication, protection, and metering devices. DERs consist of distributed generation facilities called distributed generators (DGs), which are mainly renewable and help decentralize power generation; and energy storage systems (ESSs) to store the excess of generated RE and ensure the continuous supply of critical loads in difficult circumstances. The second microgrid component includes the loads, which are generally classified into two categories of either (1) fixed or variable/flexible and (2) critical or non-critical. In terms of power management, the first classification appears considerably appropriate because fixed

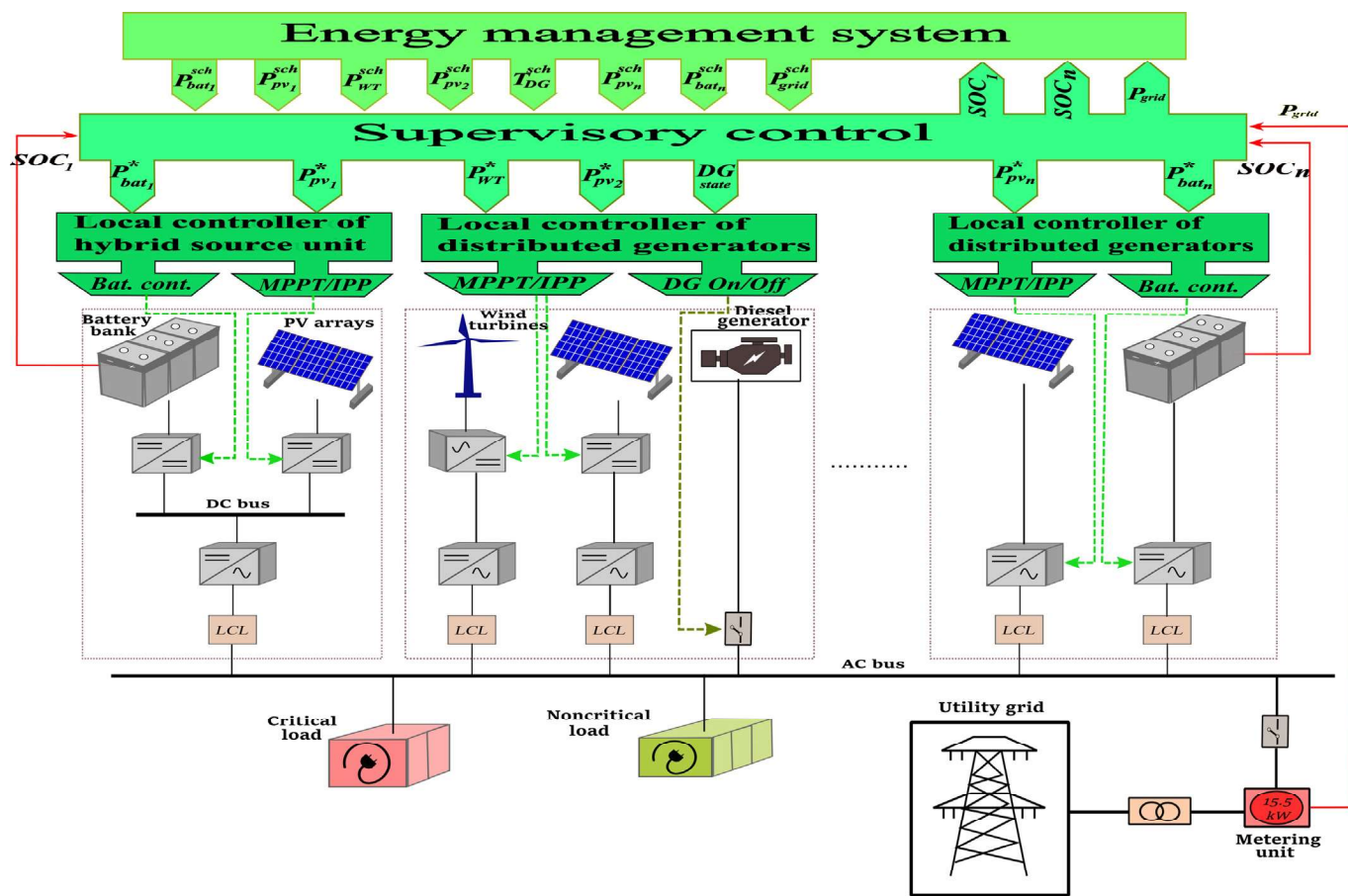


Fig. 1. Structure and control configuration of a microgrid.

loads must be satisfied under normal microgrid operation conditions, while flexible loads could be curtailed or deferred according to the microgrid power management algorithm strategy and purpose [6]. Variable loads increase the power imbalance in microgrids, which should be continuously restored by the power management algorithm. However, the second classification is considerably appropriate for the load itself, and the critical loads require a continuous and instantaneous power supply, while the non-critical loads can be shifted to work at the appropriate power generation time [33]. The third part of microgrids is the control architecture, which can be centralized or distributed. The distributed architecture is considered the high appropriate means for power controlling and power sharing between the high number of DGs, which are spread over the vast area, and have a limited communication connections and computing facilities [34,35]. This control architecture has a hierarchical structure that includes three levels: primary, secondary, and tertiary levels. The primary control level presented by local controllers (see Fig. 1) ensures the power, voltage, and frequency regulation, while the power quality and compensation of the voltage/frequency deviations are ensured by the secondary control level, in addition to the grid synchronization in the case of the grid-connected mode. The tertiary control level, which can manage single or multiple microgrids, guarantees adequate power sharing among the different DG units and power exchange between the microgrid and utility grid, will regulate power flow and maintain system stability [36].

3. Power management strategy in a microgrid

Microgrids can operate in a grid-connected mode or in islanded mode and can shift between them as well. The increased integration of RE sources in this system is accompanied by the use of energy storage system and/or back-up sources to address their intermittent nature. This multi-source topology, which can work under different modes, complicates the role of the power management algorithm, which has to share the load among the different units, considering the power generation capability of each source and maintaining the power balance of the entire system [37], either in centralized or decentralized power management. To achieve the stated power management goals, the algorithm must ensure the accomplishment of the following tasks [38].

- If the generated power is less than that requested, then all DG units are controlled to operate at their rated capacity. Moreover, if they fail to cover the demand, then the storage system intervenes to generate the lack of power. If the latter is unable to respond, then the management algorithm solicits the backup system or proceeds to the shedding solution.
- In the case when the generated power exceeds the demand, all surplus power is stored in the non-fully charged storage system or injected to the utility grid, depending on the applied mode.
- When the generated power continues to be greater than that required and the storage system is fully charged, power

curtailment must be applied by the power management algorithm to maintain the power balance. In this particular case, the application of this measure does not have to affect all DGs, and the dynamics of the source itself should be considered. Evidently, the PV source can respond rapidly to power curtailment without any influence on its physical component, but the case is different for the wind system. Accordingly, DGs should be prioritized in this mode of operation according to their dynamics.

3.1. PV unit operating modes in a microgrid

The integration of PV sources in microgrids has attracted considerable attention because they can be easily installed everywhere and require minimal maintenance cost. To adapt this source to the power management strategy of microgrids detailed in the previous sections, it must be controlled to do the following tasks:

- Shift between MPM and IPM that allow to reach the rated capacity and power curtailment, respectively;
- Rapidly alternate from one mode to another under uniform and partially shaded condition, which is caused in a real environment by clouds or neighboring buildings; and
- Enable the PV source to adapt to all operating modes of microgrids and respond to the power management controller under all working circumstances.

Achieving this objective will strengthen and improve the position of MPVS in microgrids and facilitate its integration. Under uniform irradiance, each IPP, which represents every point below MPP, has two voltages. Under the partially shaded conditions, the number of IPPs varies between two and six points, which will be detailed in the next section.

4. PV array under uniform and partially shaded conditions

To meet the rated power for MPVS, the PV panels must be connected in series and/or parallel. The series connection increases the output voltage, whereas the parallel connection increases the PV array output current. To obtain a precise modeling of the PV array that emulates the real one, the PV cell model must reproduce the real I - V characteristic curve. In the literature, single and double diodes are the most used models [39]. The first model is simple and less complex compared with the double diode model that gives more accurate results but with computation complexity. Moreover, using the one diode model to show the partial shading effect is more convenient, and gives sufficient results with minimal complexity.

When the PV array modules are exposed to non-uniform irradiation, its power-voltage (P - V) characteristics exhibit multiple peaks. The highest peak is called the global maximum point and the others are the local maximum points. Under this type of irradiation, two aspects should be mentioned and clarified: the number of peaks depends on the number of panels that receives a different irradiance level, and the position of the global maxima (GM) is linked to the irradiance intensity and the location order of the panel [29]. To illustrate this phenomena, three panels have been connected in series and exposed to uniform and non-uniform irradiance thereafter, in which the irradiance level is different for the three panels.

Fig. 2 shows the results of exposing the three panels to the same irradiance (i.e., 1 kW/m^2). Under this condition, the entire produced current flows only through the panels. Consequently, the P - V characteristics develop only one MPP.

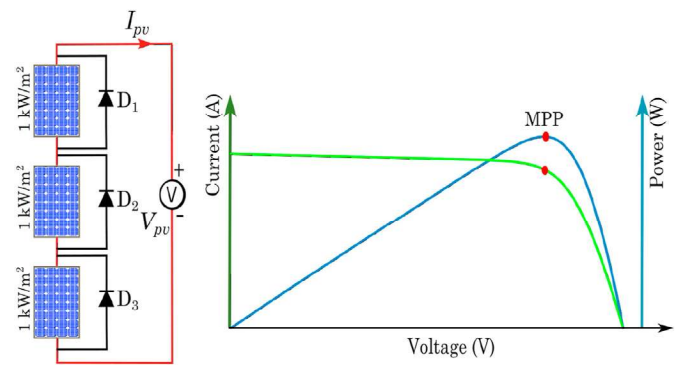


Fig. 2. PV array characteristics under uniform irradiance.

With regard to the non-uniform irradiance, Fig. 3 depicts how the three different irradiance levels develop three peaks, one GM and two LM. Furthermore, the disparities between the irradiance levels have permitted the GM to change its location: on the left side for the 1000 , 350 , and 250 W/m^2 levels (Fig. 3(a)); in the middle for the 1000 , 700 , and 350 W/m^2 levels (Fig. 3(b)); and on the right for the levels 1000 , 700 , and 500 W/m^2 levels (Fig. 3(c)).

4.1. IPPs under non-uniform condition

The irradiance level (including the partial shading case) and requested power from MPVS are not predictable. Consequently, the supervisory PV power reference P_{pv}^* may vary from small values up to the GM point. Under the partial shading conditions, the same power level also has different IPPs, as illustrated in Fig. 4. These IPPs require other techniques and algorithms, other than the MPPT algorithms, to respond precisely to the entire system supervisory request. Thus, if the supervisory power reference P_{pv}^* is not that of GM, then the intermediate power may have two, four, or even six points of the same power.

5. Proposed system description

To make the control of MPVS considerably effective in this study, which will smoothen its injection in any type of microgrid, and to allow it to respond precisely to the microgrid supervisory under any circumstances, its overall control is developed, starting with the tracking of the GM or the attaining of the IPP, until the injection of the produced power to the utility grid. Fig. 5 shows all the blocks of this MPVS. The PV generator is connected to the boost converter used to track GM or attain IPP, which itself is connected to the DC bus. The AC side begins with the three-phase voltage source inverter (VSI) used to convert the DC voltage to the AC sinusoidal voltage. The L filter at the output of VSI is used to reduce the output current distortion, while the three-phase star-delta transformer is used to isolate and boost the AC voltage level to reach that of the utility grid. Eventually, a three phase switch is used to alternate the produced power between feeding the AC load and being injected into the utility grid. For the control of the DC/DC and DC/AC converters, all the mentioned blocks, including the used methods, will be detailed in the following section.

6. Control algorithms and strategies

6.1. Boost inverter control

To allow MPVS to fulfill the requirement of any microgrid supervisory, the PV generator is controlled to instantly shift between

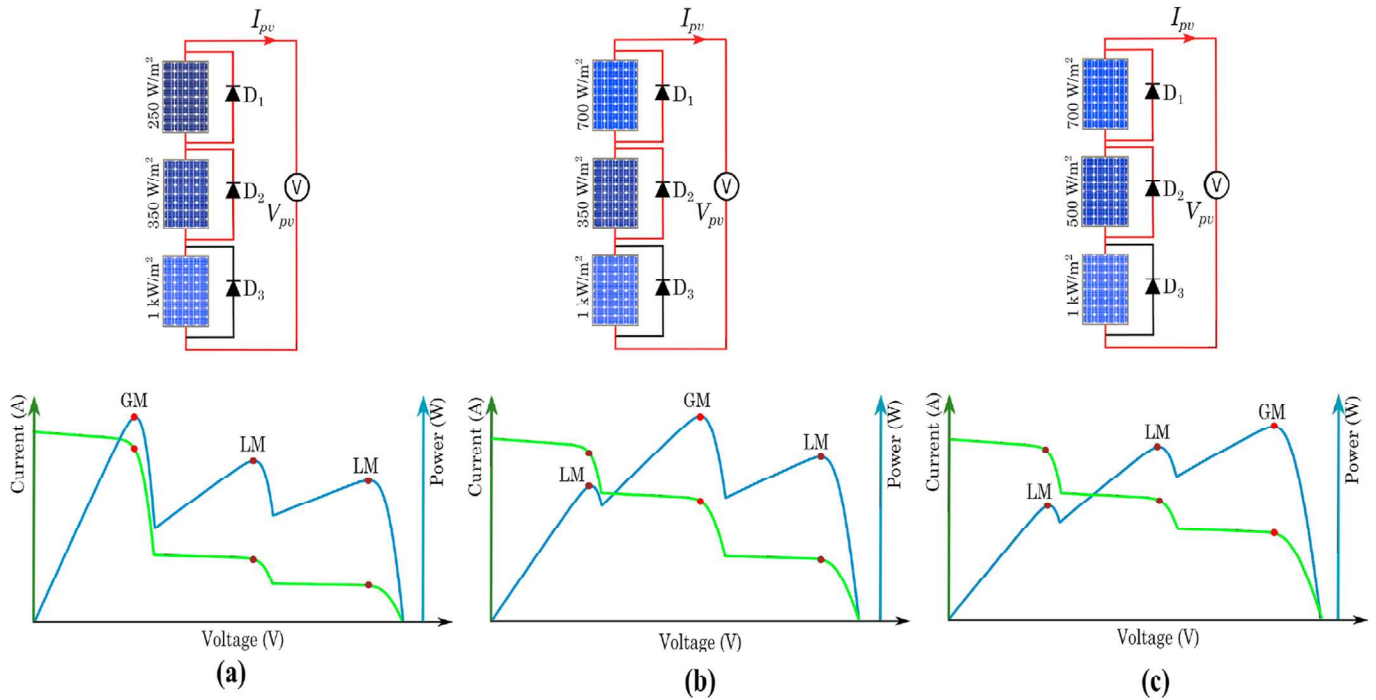


Fig. 3. PV array characteristics under uniform irradiance.

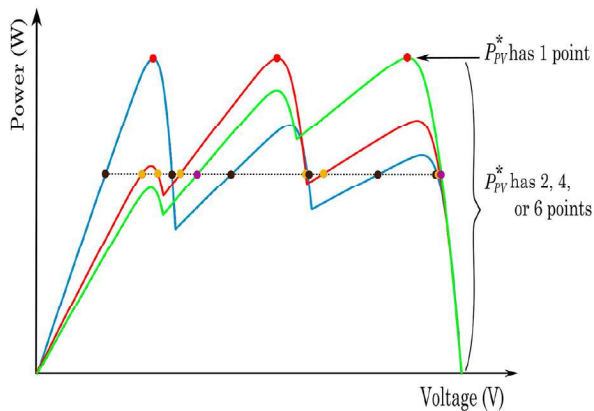


Fig. 4. PV array characteristics under non-uniform irradiance.

MPM and IPM as soon as the mode selection signal is received. For the first mode, the PSO algorithm has been selected among other swarm intelligence algorithms to track GM owing to its minimal computational complexity, which often takes time and requires more advanced implantation platform, as well as its rapid and precise GM tracking [40]. For the second mode, which makes it possible to reach any power value below GM, the IPPT algorithm is applied. The working principle of the two algorithms is detailed in the following sections.

6.1.1. PSO overview and GM tracking mechanism

PSO is one of the swarm intelligence algorithms, and is based on the positioning of particles in the search space of the optimization problem called solution candidates. For each iteration, the inter-communication and intercooperation of these particles push them toward the true solution (GM) and prevent any particle from being trapped in the illusory solution (LM). If the initial positions of these particles are X_i^0 , then their positions at next iteration X_i^1 will be

determined according to the experiences and results obtained by all the particles of the first iteration, among others. Their experiments at each iteration will be encompassed in the velocity V_i , which permits to calculate the new positions of the particles as follows:

$$X_i^{k+1} = X_i^k + V_i^{k+1} \quad (1)$$

where $i = 1, 2, \dots, Np$ is the number of particles and k represents the number of iterations.

The new velocity V_i^{k+1} is updated on the basis of the previous experiments of all the particles, including other parameters, as expressed in the following equation:

$$V_i^{k+1} = \omega V_i^k + c_1 r_1 (P_{best,i} - X_i^k) + c_2 r_2 (G_{best} - X_i^k) \quad (2)$$

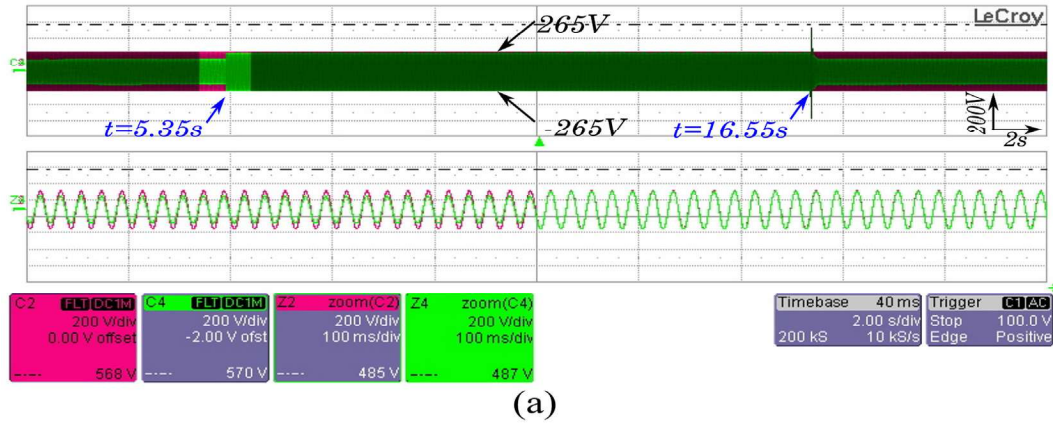
where:

- ω is the inertia weight factor;
- c_1 and c_2 are the individual particles' cognitive and social coefficients, respectively, of all particles;
- r_1 and r_2 are random variables with values that vary between 0 and 1;
- $P_{best,i}$ is the best particle that represents the best position X_i experienced by each particle during its previous iteration; and
- G_{best} is the global best that gives the best position X_i experienced among all particles during their previous iteration.

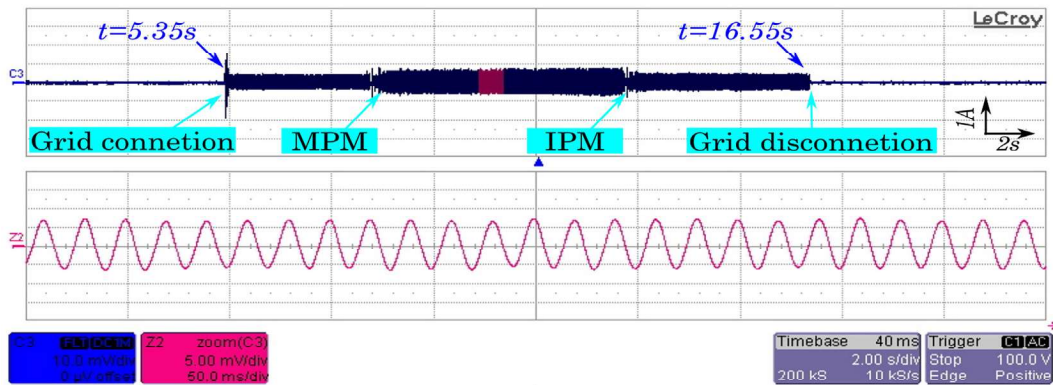
In this study, the number of particles is chosen equal to the number of peaks, while their initial values are chosen equal to 65% of the open voltage V_{oc} of each panel, thereby accelerating the tracking without the risk of missing the GM point.

6.1.2. IPPT algorithm overview and working mechanism

The IPPT algorithm allows to reach any power value other than GM, and it permits to choose IPP of the highest voltage and lowest



(a)



(b)

Fig. 15. Voltage and current with zoom of the PV unit in PPC for the first profile.

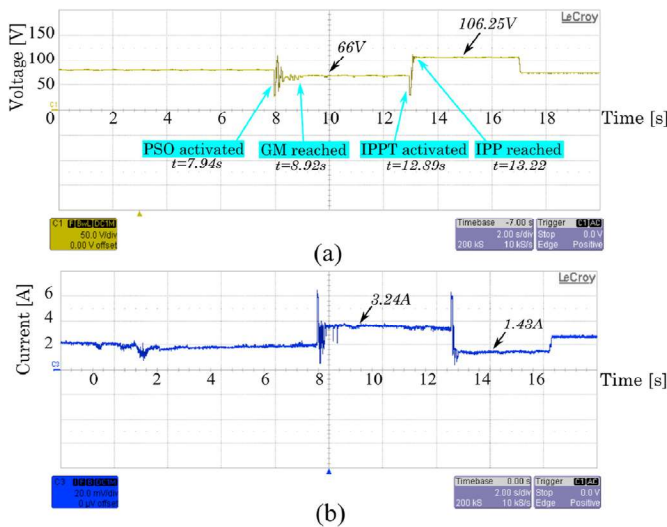


Fig. 16. Voltage and current of the middle GM profile.

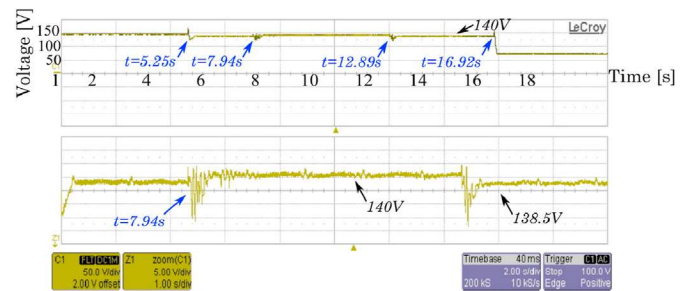


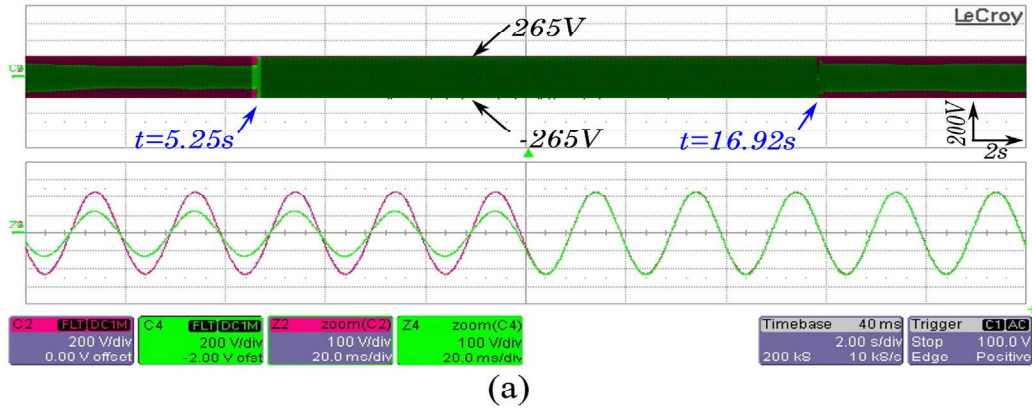
Fig. 17. Second profile of the DC bus voltage with zoom.

7.3. Discussions

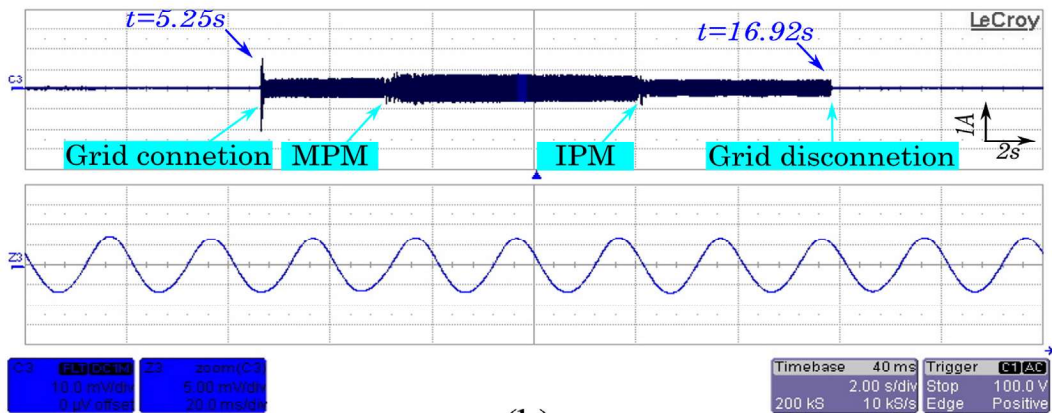
Table 2 summarizes the numerical performance results of the control algorithms during the two modes and across the three cases. The IPPT algorithm has a rapid tracking speed compared with the PSO technique, while it has less accuracy related to the power reference of the limited power, which was set close to the power of the GMPP, particularly in the right GM profile. The inclination in the

slope between the two points (i.e., GMPP and IPP) was also substantial. Moreover, the DC bus voltage decreased slightly in the limited power mode owing to the significant decrease in the DC power in this mode.

Notice that the switching between the two modes was considerably smooth, even within the challenging set goals, including the reduction of the power losses, which are achieved by choosing IPP of the highest voltage and lowest current among other points of the same power. Notice that in Case 1, the operating point shifted from the point (183.6 W/32.5 V), which corresponds to GM; to the point (126.3 W/103.53 V), which corresponds to IPP, thereby bypassing five points (20.7, 39.3, 50.2, 74.5, and 80 V) of the same power value (≈ 126 W). Similarly, the operating point in Case 2 moved from GM (213.9 W/68.6 V) to IPP (152 W/106.25 V) bypassing two points (76 V/81.7 V). For Case 3, GM and IPP are close to each other. Furthermore, another notable feature of the IPPT algorithm is that



(a)



(b)

Fig. 18. Voltage and current with zoom of the PV unit in PPC for the second profile.

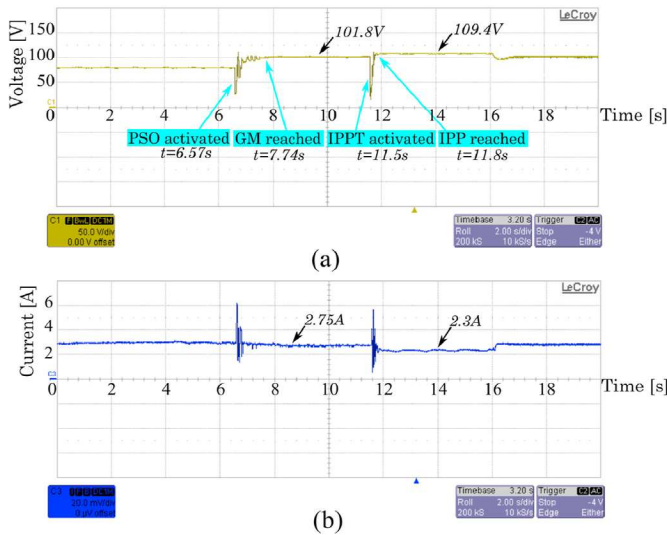


Fig. 19. Voltage and current of the left side GM profile.

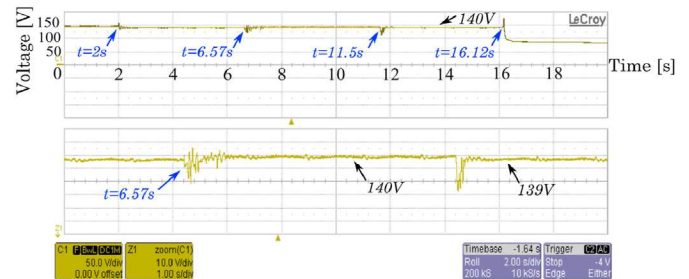


Fig. 20. Third profile DC bus voltage with zoom.

once IPP is found, the V_{mp} value is held constant, which has eliminated the steady-state oscillations of the voltage V_{PV} , thereby reducing the power loss and enhance system performance. Evidently, the DC bus voltage at the inverter input is stably maintained at approximately 140 V. This result was achieved despite the large V_{PV} voltage gap for the two points (i.e., GM and IPP), specifically for Case 1 and with less impact in Case 2.

As discussed in the DC side results, the IPPT algorithm is robustly capable of achieving any desired power reference lower than the

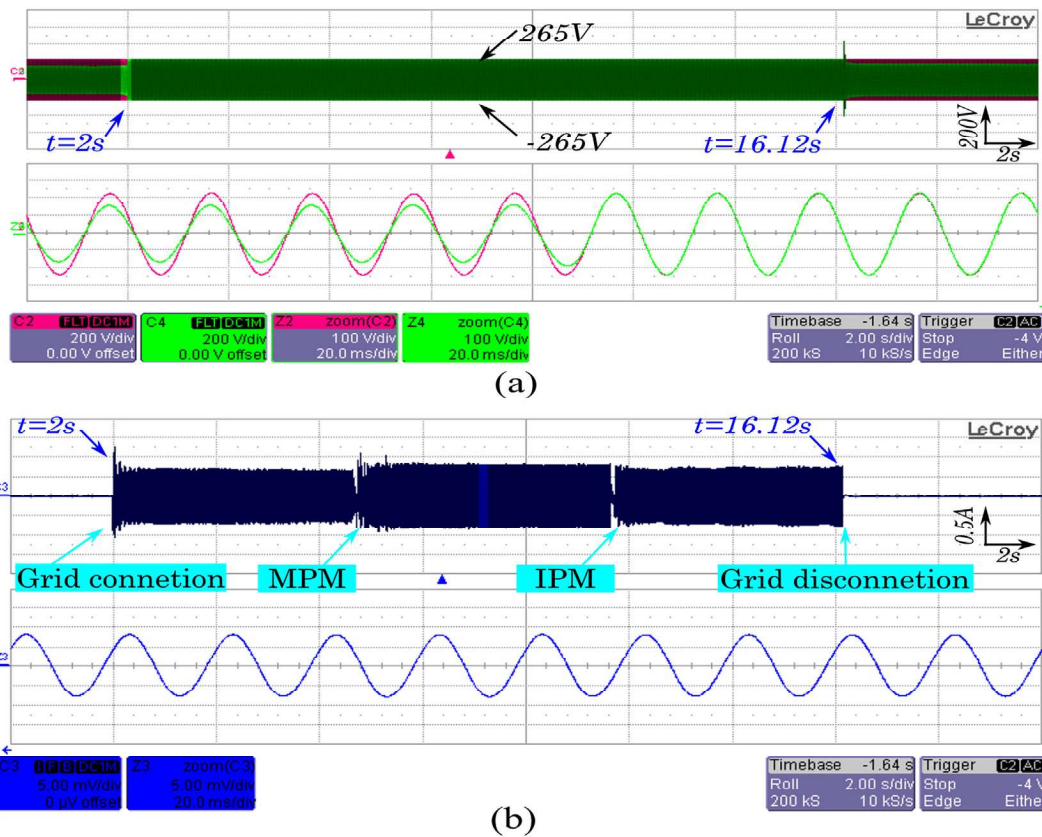


Fig. 21. Voltage and current with a zoom of the PV unit in PPC for the third profile.

3 Phase 300V LOCAL		OUT		
OUTPUT SETTING				Main
#1	V _{ac} = 110.0V	F = 50.00Hz		OUTPUT: More Setting
#2	V _{ac} = 110.0V	F = 50.00Hz		Measurement Setting
#3	V _{ac} = 110.0V	F = 50.00Hz		Waveform Viewer
MEASUREMENT				Limitation
#1	V = 110.05	P _o = -61.1		Output Mode
	I = 0.572	PF = -0.970		Measurement To Page2
#2	V = 110.01	P _o = -60.3		
	I = 0.564	PF = -0.972		
#3	V = 110.01	P _o = -61.1		
	I = 0.561	PF = -0.990		
	V ₁₂ = 190.56	V ₂₃ = 190.58		
	V ₃₁ = 190.70	P _o = -182.5		

Fig. 22. Screenshot of the grid emulator Chroma 61511.

MPP power, with considerable precision and speed regardless of the irradiance profile. Maintaining the DC bus voltage constant, even with rapid voltage variations during the tracking period and mode-shifting, verifies the effectiveness and validates the performance of the VOC strategy in the three-phase VSI control.

At PCC, the synchronization process was successful owing to the

PLL technique. During the power injection interval, the PV unit and grid emulator voltages were completely overlapped. Outside of this interval, they are in phase with different amplitudes. However, the current and voltage waveforms are in a phase opposition owing to the power injection. Note that at the AC side, the system underwent two test scenarios: resistive load supply and power injection. Nevertheless, the first scenario has no amplitude voltage regulation, thereby proving the capability of the system, with and without operating point control, to switch to and from the power injection mode; and to maintain the DC bus voltage constant despite the disturbances occurring during the operating points tracking and the mode shifting.

After discussing the results of the different cases, the experimental validation confirms the ability of MPVS to respond successfully to the dual control technique even under the challenging conditions will eliminate the power control limits of this system, expand its penetration, and strengthen its role inside the microgrid. By contrast, it ensures the optimum performance of the IPPT algorithm whether for speed tracking or efficiency.

Lastly, the efficiency and reliability of the proposed MPVS, in terms of topology and control, are summarized in Table 3. The first column outlined the properties and advantages of this unit, while

Table 2 Summary of the numerical values of the experimental results of the three case studies.

Cases	Power values		Search time for		Error percentage in		DC bus voltage during	
	GMPP	IPP	PSO	IPPT	GMPP	IPP	GMM	IPM
Left GM profile	183.5W	120W	1.5s	0.2s	0.07%	5.25%	140V/0%	138V/1.42%
Middle GM profile	213.9W	150W	0.98s	0.33s	0.03%	1.29%	140V/0%	138.5V/1.07%
Right GM profile	269.4W	230W	1.17s	0.3s	2.88%	9.4%	140V/0%	139V/0.71%

Table 3
Summary of the proposed PV unit's properties and advantages with the obtained results.

Properties/Advantages	Achieved results
Ease of insertion into a microgrid whatever the working conditions could be.	<ul style="list-style-type: none"> • Ability to switch smoothly and rapidly between the two modes (i.e., MPM and IPM); • Guarantee of minimal power loss in IPM; • The possibility of operating in grid-connected or islanded mode; • Ability of being interconnected with other sources via the DC bus.
Work under partial shading mode. Considerably rapid response to the supervisory.	<ul style="list-style-type: none"> • Convincing results were obtained under different partial shading mode patterns. • For MPM, the tracking time varies between 0.98 s and 1.17 s. • For IPM, the searching time varies between 0.2 s and 0.33 s.
Precise response to the supervisory.	<ul style="list-style-type: none"> • GM was reached with error varying between 0.03% and 2.88%. • IPP was reached with error varying between 1.29% and 9.4%.
Good stability of the DC bus voltage.	<ul style="list-style-type: none"> • The DC bus voltage was maintained constant despite the challenging test conditions, while its voltage reference was achieved with an error rate varied between 0.7% and 1.4%.
Good power factor value. Hardware implementation simplicity of the used algorithms	<ul style="list-style-type: none"> • The power factor varies between 0.95 and 0.99. • The PSO, IPPT, and VOC algorithms requires minimal computation time, thereby reducing the implementation cost

the second column describes the achieved results.

Research Grant Scheme (FRGS): FRGS/1/2020/TK0/UM/02/15.

8. Conclusion

This study developed a novel integral control strategy for MPVS to strengthen its role in microgrid systems, facilitate its integration, and increase its efficiency. The main findings can be presented as follows.

- The two-stage topology is the most appropriate method to interconnect the components of MPVS because it allows for eventual sharing of the DC bus with the storage system or with other distributed generation units.
- The smooth switching between the two modes (i.e., MPM and IPM) enables the efficient use of MPVS and increases its reliability, as it is able to fulfill all modern microgrid supervisory requirements.
- The proposed IPPT algorithm is used to track the intermediate power points under the partially shaded conditions. Apart from achieving the precise power reference, it also has the ability to choose the least current IPP among other points of the same power.
- The expected results from MPVS were verified experimentally. Thus, under three partial shading profiles that exposed different GM point locations, the PV unit has successively switched between the two modes, and responded rapidly and accurately to the supervisory requirements while maintaining the DC bus voltage constant.
- Compared with the PSO technique, the IPPT algorithm has given convincing results, while succeeding in reaching IPP in an average time of 0.26 s versus PSO, which took an average time of 1 s to reach GMPP.

Further research may investigate the replacement of the three-phase two-level inverter with multilevel inverter, and propose a new control technique that addresses microgrid disturbances.

Declaration of competing interest

The authors declare that they have no known competing financial interests or personal relationships that could have appeared to influence the work reported in this paper.

Acknowledgement

The authors would like to thank the Ministry of Higher Education, Malaysia, for the financial support under the Fundamental

References

- [1] Breyer C, Vainikka P, Aghahosseini A, Solomon A. Solar photovoltaics demand for the global energy transition in the power sector. *Prog. photovoltaics* 2017;(August):1–19. <https://doi.org/10.1002/PIP.2950>.
- [2] Isa NM, Das HS, Tan CW, Yatim AHM, Lau KY. A techno-economic assessment of a combined heat and power photovoltaic/fuel cell/battery energy system in Malaysia hospital. *Energy* 2016;112:75–90. <https://doi.org/10.1016/j.energy.2016.06.056>.
- [3] Child M, Koskinen O, Linnanen L, Breyer C. Sustainability guardrails for energy scenarios of the global energy transition. *Renew Sustain Energy Rev* 2018;91(April 2017):321–34. <https://doi.org/10.1016/j.rser.2018.03.079>.
- [4] Almezahia AA, Al-Masri HM, Ehsani M. Integration of renewable energy sources by load shifting and utilizing value storage. *IEEE Transactions on Smart Grid* 2018;10(5):4974–84.
- [5] United States Department of Energy. *How microgrids work*. 2014.
- [6] Parhizi S, Member S, Lotfi H, Member S. State of the art in research on microgrids. *A Review* 2015;3536(c):1–37. <https://doi.org/10.1109/ACCESS.2015.2443119>.
- [7] Newman S, Shiozawa K, Follum J, Barrett E, Douville T, Hardy T, Solana A. A comparison of pv resource modeling for sizing microgrid components. *Renew Energy* 2020;162:831–43.
- [8] Zolfaghari M, Hosseinian SH, Fathi SH, Abedi M, Gharehpetian GB. A new power management scheme for parallel-connected pv systems in microgrids. *IEEE Transactions on Sustainable Energy* 2018;9(4):1605–17.
- [9] Li G, Jin Y, Akram MW, Chen X, Ji J. Application of bio-inspired algorithms in maximum power point tracking for PV systems under partial shading conditions – a review. *Renew Sustain Energy Rev* 2018;81(May 2017):840–73. <https://doi.org/10.1016/j.rser.2017.08.034>.
- [10] Li H, Member S, Yang D, Su W. An overall distribution particle swarm optimization MPPT algorithm for photovoltaic system under partial shading. *IEEE Trans Ind Electron* 2018;66(1, Jan. 2019):265–75. <https://doi.org/10.1109/TIE.2018.2829668>.
- [11] Mohanty S, Subudhi B, Member S, Ray PK. A new MPPT design using grey wolf optimization technique for photovoltaic system under partial shading conditions. *IEEE Trans. Sustain. ENERGY* 2016;7(1):181–8.
- [12] Peng B-R, Ho K-C, Liu Y-H. A novel and fast mppt method suitable for both fast changing and partially shaded conditions. *IEEE Trans Ind Electron* 2017;65(4):3240–51.
- [13] Inci M, Caliskan A. Performance enhancement of energy extraction capability for fuel cell implementations with improved cuckoo search algorithm. *Int J Hydrogen Energy* 2020;45(19):11309–20.
- [14] Yang B, Zhong L, Zhang X, Shu H, Yu T, Li H, Jiang L, Sun L. Novel bio-inspired memetic salp swarm algorithm and application to MPPT for PV systems considering partial shading condition. *J Clean Prod* 2019;215:1203–22. <https://doi.org/10.1016/j.jclepro.2019.01.150>.
- [15] Benyoucef AS, Chouder A, Kara K, Silvestre S, Sahed OA. Artificial bee colony based algorithm for maximum power point tracking (MPPT) for PV systems operating under partial shaded conditions. *Appl Soft Comput J* 2015;32:38–48. <https://doi.org/10.1016/j.asoc.2015.03.047>.
- [16] Sundareswaran K, Peddapati S, Palani S. MPPT of PV systems under partial shaded conditions through a colony of flashing fireflies. *IEEE Trans Energy Convers* 2014;29(2):463–72.
- [17] Lian L, Maskell DL, Patra JC. A novel ant colony optimization-based maximum power point tracking for photovoltaic systems under partially shaded conditions. *Energy Build* 2013;58:227–36. <https://doi.org/10.1016/j.enbuild.2012.12.001>.
- [18] Yang B, Yu T, Zhang X, Li H, Shu H, Sang Y, Jiang L. Dynamic leader based collective intelligence for maximum power point tracking of pv systems

- affected by partial shading condition. *Energy Convers Manag* 2019;179:286–303.
- [19] Eltamaly AM, Farh HM. Dynamic global maximum power point tracking of the pv systems under variant partial shading using hybrid gwo-flc. *Sol Energy* 2019;177:306–16.
- [20] Ahmad R, Murtaza AF, Sher HA. Power tracking techniques for efficient operation of photovoltaic array in solar applications—a review. *Renew Sustain Energy Rev* 2019;101:82–102.
- [21] Yang Y, Wang H, Blaabjerg F, Kerekes T. A hybrid power control concept for PV inverters with reduced thermal loading. *IEEE Trans Power Electron* 2014;29(12):6271–5. <https://doi.org/10.1109/TPEL.2014.2332754>.
- [22] Sangwongwanich A, Yang Y, Blaabjerg F. High-performance constant power generation in grid-connected PV systems. *IEEE Trans Power Electron* 2016;31(3):1822–5.
- [23] Choudar A, Boukhetala D, Barkat S, Brucker J-M. A local energy management of a hybrid PV-storage based distributed generation for microgrids. *Energy Convers Manag* 2015;90:21–33. <https://doi.org/10.1016/j.enconman.2014.10.067>.
- [24] Golsorkhi MS, Member GS, Shafiee Q, Lu DDC, Member S. A distributed control framework for integrated photovoltaic-battery based islanded microgrids. *IEEE Trans Power Electron* 2017;8(6):2837–48. <https://doi.org/10.1109/TSG.2016.2593030>.
- [25] Kim M, Bae S. Decentralized control of a scalable photovoltaic (PV) -battery hybrid power system. *Appl Energy* 2017;188:444–55. <https://doi.org/10.1016/j.apenergy.2016.12.037>.
- [26] Gassab S, Radjeai H, Mekhilef S. Power management and coordinated control of standalone active PV generator for isolated agriculture area-case study in the South of Algeria Power management and coordinated control of standalone active PV generator for isolated agriculture area-case study. *J Renew Sustain Energy* 2019;11(1):1–13. <https://doi.org/10.1063/1.5064444>.
- [27] Ahmad R, Murtaza AF, Ahmed H. Power tracking techniques for efficient operation of photovoltaic array in solar applications – a review. *Renew Sustain Energy Rev* 2019;101(November 2017):82–102. <https://doi.org/10.1016/j.rser.2018.10.015>.
- [28] Belhachat F, Larbes C. Comprehensive review on global maximum power point tracking techniques for pv systems subjected to partial shading conditions. *Sol Energy* 2019;183:476–500.
- [29] Guichi A, Talha A, Berkouk EM, Mekhilef S, Gassab S. A new method for intermediate power point tracking for PV generator under partially shaded conditions in hybrid system. *Sol ENERGY* 2018;170(February):974–87.
- [30] Kadri R, Gaubert JP, Champenois G. An Improved maximum power point tracking for photovoltaic grid-connected inverter based on voltage-oriented control. *IEEE Trans Ind Electron* 2011;58(1):66–75. <https://doi.org/10.1109/TIE.2010.2044733>.
- [31] Yang B, Yu T, Shu H, Zhu D, Zeng F, Sang Y, Jiang L. Perturbation observer based fractional-order pid control of photovoltaics inverters for solar energy harvesting via yin-yang-pair optimization. *Energy Convers Manag* 2018;171:170–87.
- [32] Department of Energy Office of Electricity Delivery and Energy Reliability, Summary Report : 2012 DOE Microgrid Workshop, Tech. rep., Department of Energy Office of Electricity Delivery and Energy Reliability, Available: <http://energy.gov/sites/prod/files/2012.Microgrid.Workshop.Report.09102012.pdf>. [Accessed: 10-Oct- 2019].
- [33] Ayodele TR, Ogunjuyigbe ASO, Akpeji KO, Akinola OO. Prioritized rule based load management technique for residential building powered by PV/battery system. *Eng. Sci. Technol. an Int. J.* 2017;20(3):859–73. <https://doi.org/10.1016/j.jestch.2017.04.003>.
- [34] A. Karaarslan, M. E. Seker, Distributed control of microgrids, in: *Microgrid Archit. Control Prot. Methods*, Springer International Publishing, doi:10.1007/978-3-030-23723-3_16, Ch. Springer I. doi:10.1007/978-3-030-23723-3_16.
- [35] A. Dimeas, A. Tsikalakis, G. Kariniotakis, G. Korres, Microgrids control issues, in: *Microgrids Archit. Control*, Chichester, U.K.: Wiley, doi: 10.1002/9781118720677.ch02. arXiv:arXiv:1011.1669v3, doi:10.1017/CBO9781107415324.004.
- [36] Meng L, Luna AC, Diaz ER, Sun B, Savaghebi M, Juan C, Guerrero JM. Flexible system integration and advanced hierarchical control architectures in the microgrid research laboratory of Aalborg University Moises Graells. *IEEE Trans Ind Appl* 2016;52(2):1736–49. <https://doi.org/10.1109/TIA.2015.2504472>.
- [37] He J, Li YW. An enhanced microgrid load demand sharing strategy. *IEEE Trans Power Electron* 2012;27(9):3984–95. <https://doi.org/10.1109/TPEL.2012.2190099>.
- [38] Karimi Y, Oraee H, Member S, Golsorkhi MS, Student G. Decentralized method for load sharing and power management in a PV/battery hybrid source islanded microgrid. *IEEE Trans Power Electron* 2017;32(5):3525–35. <https://doi.org/10.1109/TPEL.2016.2582837>.
- [39] Belhaouas N, Cheikh MA, Agathoklis P, Oularbi M, Amrouche B, Sedraoui K, Djilali N. PV array power output maximization under partial shading using new shifted PV array arrangements. *Appl Energy* 2017;187:326–37. <https://doi.org/10.1016/j.apenergy.2016.11.038>.
- [40] Elobaid LM, Abdelsalam AK, Zakzouk EE. Artificial neural network-based photovoltaic maximum power point tracking techniques: a survey. *Renew. Power Gener. IET* 2015;9(8):1043–63. <https://doi.org/10.1049/iet-rpg.2014.0359>.